Fabrication of Cr nanoring arrays by nanosphere lithography for light extraction

HUNG-CHUN WU, HSI-HSIN CHIEN*, KUNG-JENG MA, MING-DONG BAO[a], YU-HSUAN HO[b]
College of Engineering, Chung Hua University, Hsin Chu 300, Taiwan
[a]*Institute of Materials Engineering, Ningbo University of Technology, Ningbo 315016, China*
[b]*Research Center for Applied Sciences, Academia Sinica, Taipei 11572, Taiwan*

Functional nanorings with optical and magnetic properties have attracted intensive attentions. This study aims to develop a low cost process for the fabrication of Cr nanoring arrays to improve light extraction. The Cr nanoring arrays in long-ranged hexagonal order with controllable period can be obtained by nanosphere assembly, followed by plasma etching, Cr coating and lift off processes. The effects of coating and reactive ion etching process on the size and shape of Cr nanorings were investigated. The results show that the mean values of lateral size and height of nanorings are in the range of 147.1~196.4 nm and 7.8~40.8 nm respectively. The statistical analysis shows that lateral size distribution of the Cr nanorings varied with different deposition times. In order to verify the optical effect, a 100 nm ALq3 thin film was deposited onto the nanoring arrays by thermal evaporation, and pumped the Alq3 layer with 405 nm blue laser. The phenomenon of this nano-optics gave rise to a selective spectral response and a 32.6 % extraction enhancement was observed compared to a flat substrate.

(Received August 6, 2012; accepted October 30, 2012)

Keywords: Nanoring arrays, Nanosphere lithography, Spin-coating, Reactive ion etching

1. Introduction

Functional nanorings have attracted intensive attentions recently for the unique properties and potential applications, such as optical [1], magnetic [2], sensors [3, 4], and opto-electronic devices [5, 6]. These properties are usually influenced by the shape, size and interfeature spacing. For instance, magnetic nanorings in high density magnetic recording and vertical magnetic random access memory [7, 8], metallic nanorings exhibit a localized surface plasmon that can be tuned over an extended wavelength range by varying the ratio of the ring thickness to its radius [3, 9]. T. W. Ebbesen et al. found that optical transmission was enhanced in periodic arrays of perforated Cr metallic films due to the coupling of light with surface plasmons [10-12]. Various fabrication techniques, such as X-ray lithography [13], electron-beam lithography (EBL) [14], nanoimprint lithography (NIL) [15], porous polymer membrane templating [16], and structured template techniques [17] have been developed to produce periodic metallic nanostructure array. However, these approaches have the significant limitations of being both high-cost and sophisticated. Recently more researches have focused on the development of low-cost, high-throughput, and simple nanosphere lithography (NSL) technique to fabricate periodic nanostructure arrays [18]. Several research groups have reported large-scale periodic nanostructure arrays by NSL, where colloid confinement methods [19], vertical deposition [20], and electrophoretic deposition [21] are used as coating processes. In recent years, spin-coating had been widely employed to form the 2-D hexagonal close-packed crystal-like structures of polystyrene nanospheres on glass substrates [22, 23]. The centrifugal force was used to replace the gravity force in self-assembly and formed an organized structure of nanospheres. By controlling the concentration of nanosphere solution and the rotation speed of the spin coater, a monolayer of nanospheres was spun on the substrate. The formation of the hexagonal close-packed monolayer was determined by the mixing ratio and the spinning speed.

The next step is to manipulate the size and distribution colloidal particles on the glass substrate by reactive ion etching. The followed metallic film deposition and lift off process allow periodic metallic nanorings to be formed on glass substrate. Every process parameter plays an important role to determine the morphologies of nanoring's structure. There still exist many technical challenges to precisely control the distribution and size of periodical nanoring's structure.

In this study, polystyrene nanospheres with hexagonal close-packed structure were formed on glass substrates by spin-coating method. Next, the long-range hexagonal ordered Cr nanorings on glass substrates can be produced by reactive ion etching, Cr coating and lift off process. The size and shape and distribution of Cr nanorings can be

manipulated by Cr coating and reactive ion etching (RIE) processes. Finally, the optical effect of nanoring structure was investigated by photoluminescence experiment.

2. Experimental

The polystyrene nanospheres of mean diameters of 540 nm were purchased from Bangs Laboratories Inc. in polystyrene nanospheres solution of 10 wt.% concentration. Fig. 1 shows the schematic diagram of the fabrication process for periodic metallic nanoring arrays. The four steps are as follows: (a) to form a monolayer of polystyrene (PS) nanospheres on the glass substrate by spin coating process, (b) to reduce the nanospheres by O_2 RIE process, (c) to fill the air-gap with Cr thin film by using a closed field unbalanced magnetron sputtering ion plating system (CFUBMIP), and (d) to form Cr nanoring arrays by lift-off process.

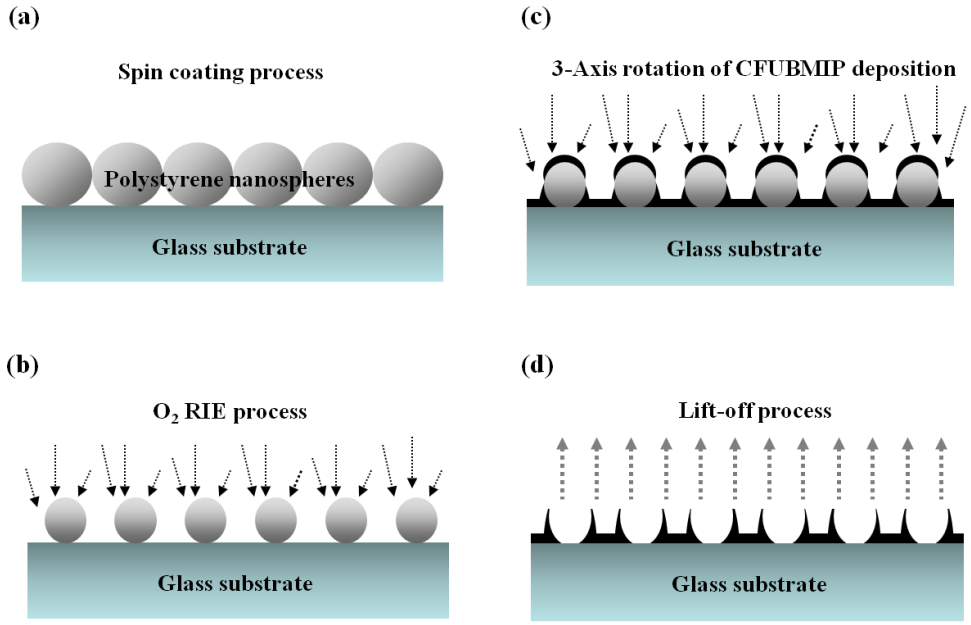

Fig. 1. Schematic diagrams of nanosphere lithography: (a) a monolayer of polystyrene nanospheres is formed on the clean glass substrate by spin coating process. (b) Reduce the nanospheres by oxygen plasma etching. (c) Using a closed field unbalanced magnetron sputtering ion plating system (CFUBMIP) to deposit the metal to fill in the gap between nanospheres. (d) After the lift-off process, the periodic metallic nanoring is formed.

In order to successfully prepare the hexagonal monolayer, it is necessary to prepare a hydrophilic surface on the glass substrates. First, the square glass substrates of 15 mm ×15mm were initially cleaned and submerged in a 1:1 mixture of NH_4OH and hydrogen peroxide (H_2O_2) solution for 30 min in ultrasonic bath, and then rinsed with deionized water for 5 min in ultrasonic bath. These approaches would add many –OH groups on the glass surface, which make the substrates to be hydrophilic and help form a monolayer of polystyrene (PS) on it. A standard spin-coater was used to coat the dispersion onto glass substrates. At a speed of 1200 rpm for 4 minutes, the hexagonal close-packed structures were formed. The period of this hexagonal array was determined by the diameter of polystyrene spheres. The size of nanosphere was controlled by the isotropic O_2 RIE process with RF power of 50W for 5 min and followed by a lower plasma power of 30 W for 16 min. Subsequently, a CFUBMIP system (CFUBMIP, Huijin Teer Coatings Ltd, UDP650) was used to fill the air-gap with Cr thin film. The sputtering target was pure metal Cr (99.99%). During deposition, the samples were mounted on the three-axis rotation jigs with a speed of 4 rpm. The distance between substrates and targets was 150 mm. After the sputtering chamber was pumped to the base pressure of 1.5×10^{-5} torr, high-purity argon gas with a flow rate of 25 sccm was introduced into the chamber from mass flow controller, wherein a DC bias voltage of 500 V was applied to the substrate and 0.5A current applied on Cr targets, resulting in an overall circular symmetric deposition flux. After deposition of Cr thin film, the PS nanospheres were completely removed in dichloromethane (CH_2Cl_2) solution and vibrated with ultrasonic cleaner for 5 min. Dichloromethane was used to dissolve and lift off the PS nanospheres. Then the samples were treated with acetone (CH_3COCH_3) and ethanol (C_2H_5OH) in the same way. The Cr nano-ring arrays with well-ordered two-dimensional periodic structures will be obtained eventually.

The surface and cross-sectional morphology of the Cr nanoring arrays were observed by using a Hitachi S-4800 Cold Field Emission SEM. Topography of the Cr nanoring arrays were measured by using an atomic force microscopy (AFM; NanoScope III System Digital Instrument) in the tapping mode to measure the surface profile of the Cr nanoring arrays. A diode laser of wavelength 405 nm was used as pumping source at the normal direction in the photoluminescence experiment. The excellent beam characteristics such as mode quality and low divergence made the laser suitable for beam focusing, as well as long distance beam positioning. Laser passed through a pin hole and convex lenses, focused on the device chip. Organic light emitters were pumped by laser directly, and the photoluminescence was detected with scanning at 45 degree incident angle. The emission of organic film on nanorings array film was collected by a focal lens and analyzed by the spectrum meter.

3. Results and discussion

SEM morphologies of spin-coated PS nanosphere before and after RIE etching were successfully fabricated by a self-assembly process, as shown in Fig. 2. The usual way of reducing the diameter of PS colloidal nanosphere is thinned by RIE in O_2 atmosphere process [24]. From Fig. 2 (a) and (b), it can be observed that high-quality long-ranged ordered monolayer of PS nanosphere arrays can be formed by spin-coating method. The PS nanosphere possesses a smooth surface with a diameter of 540 nm. After the closed-packed monolayer was formed, the size of the polystyrene nanosphere mask can be further reduced by RIE in O_2 atmosphere process with a RF power of 50 W for 5min, and then 30 W for 16 min as shown in Fig. 2 (c) and (d). The high-quality long-ranged periodic monolayer of polystyrene nanosphere arrays still can be maintained after O_2 plasma etching process. The measured diameter of nanospheres is in the range of 540 nm to 358 nm. This can be attributed to the oxygen ion will degrade the PS nanosphere surface due to the hydrogen abstraction on the polymer chain or C–C bond scission by ion bombardment, and remove the weak boundary layers during ion interaction with the Polymer [25].

The correlation between the diameter D of thinned polystyrene and etching time t obeys the following empirical equation [26]:

$$D=D_0 \cos [\text{arcsine } (kt/2D_0)] \quad (1)$$

where D_0 is the initial diameter of the PS nanosphere and k is the constant depending on the etching conditions such as pressure, incident power, gas flow, and temperature. In this paper, when etching constant of the *k* value is chosen around 0.65, the experimental data agrees well with the equation (1). Therefore, the PS nanosphere sizes can be controlled simply by varying the etching time. The period of array of PS nanosphere is determined by the initial diameter of polystyrene beads.

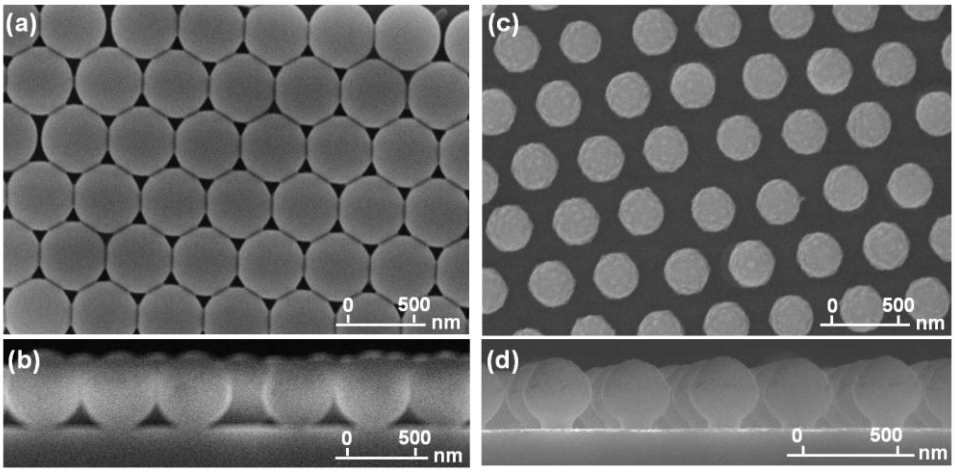

Fig. 2. (a) Top view and (b) Cross-sectional view, of SEM image of the spin coated monolayer polystyrene nanosphere arrays with 540nm diameter on the clean glass substrate; (c) Top view and (d) Cross-sectional view, of SEM image of the polystyrene nanosphere colloidal ion etched by O_2 RIE for 50W, 5min, and then 30W, 16min.

After the nanosphere mask was formed, the Cr film was deposited by CFUBMIP system to fill the air-gap between the nanospheres with a deposition time of 1 min, 3 min, and 5 min, respectively. The followed nanospheres lift-off process allows arrayed Cr nanorings with 540 nm period in long-ranged hexagonal order to be formed, as shown in Fig. 3. It can be seen that ordered patterns of polystyrene template are well transferred to the Cr nanoring arrays with uniform, distinct sidewalls. This can be attributed to the Cr atoms/ions were very well deposited into the triangular interstices among the PS nanospheres, aggregation of these Cr atoms/ions formed a ring-shaped structures tend to move under the PS nanosphere. After lift-off process the porous Cr nanoring arrays were obtained.

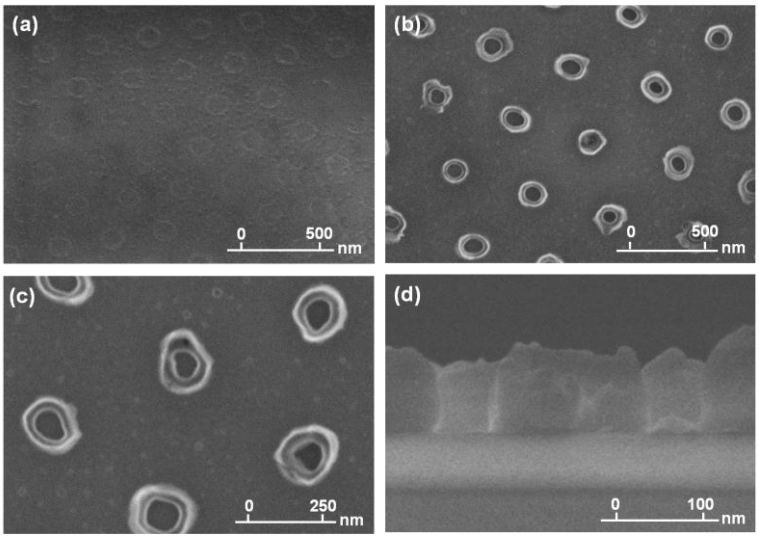

Fig. 3. SEM images of arrayed Cr nanorings prepared by nanosphere lithography where the Cr thin film with deposition duration of (a) 1min. (b) 3 min. (c) 5min. (d) high magnification of cross-sectional view of the Cr nanoring observed in (c).

AFM images in Fig. 4 (a-b) show the 3D topography surface of ordered Cr nanoring arrays processed with Cr deposition time of 1 min and 5 min respectively, and followed by O_2 RIE etching to remove of polystyrene nanosphere. It is clearly observed that all ordered patterns of polystyrene template are well transferred to the Cr surface and the Cr nanoring arrays are uniform in large area. The measured average height of the Cr nanorings is around 7.8 nm and 40.8 nm, for the samples with deposition time of 1 min and 5 min respectively. The Cr nanorings with a period of 540 nm are determined by the initial diameter of PS spheres.

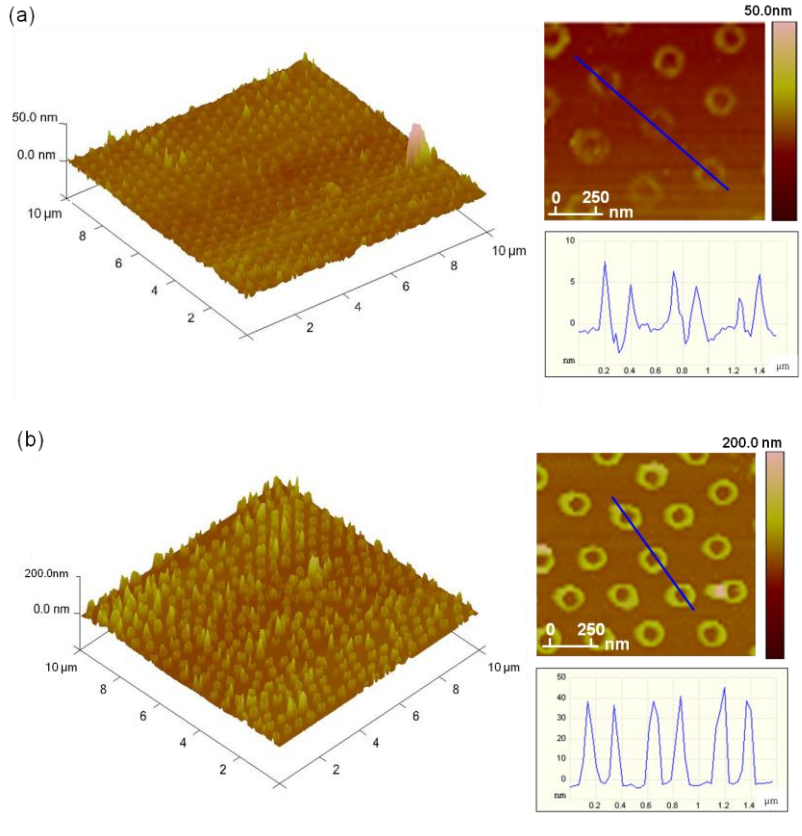

Fig. 4. AFM of 3D topography surface of ordered Cr nanoring arrays, and the mean values of cross-sectional of Cr nanoring arrays measured around (a) 7.8 nm high for Cr deposition time of 1 min. (b) 40.8 nm high for Cr deposition time of 5 min.

The distribution of lateral size of Cr nanorings varies with the deposited time, as shown in Fig. 5 (a-e). The standard deviation ΔL, the mean value of lateral size ⟨L⟩ and the dispersion δ = ΔL/⟨L⟩ are obtained. All of the data from every nanoring can be fitted by a Gaussian function and the fitting curves are also given using a red curve in every plot. The dispersion of lateral size for every Cr nanoring are plotted in Fig. 5 (f), the level of δ also be presented as a function of deposition time here. It is found that the dispersion of lateral size was increased with the increase of deposition time. Because the value of δ influenced by O_2 RIE process is only about 1.6%, it can be speculated that the size dispersion mainly caused by the deposition process of Cr thin film. The linear relationship between the mean of lateral size and deposition time will help to control the finally dimensional accuracy of nanoring prepared using magnetron sputtering approach.

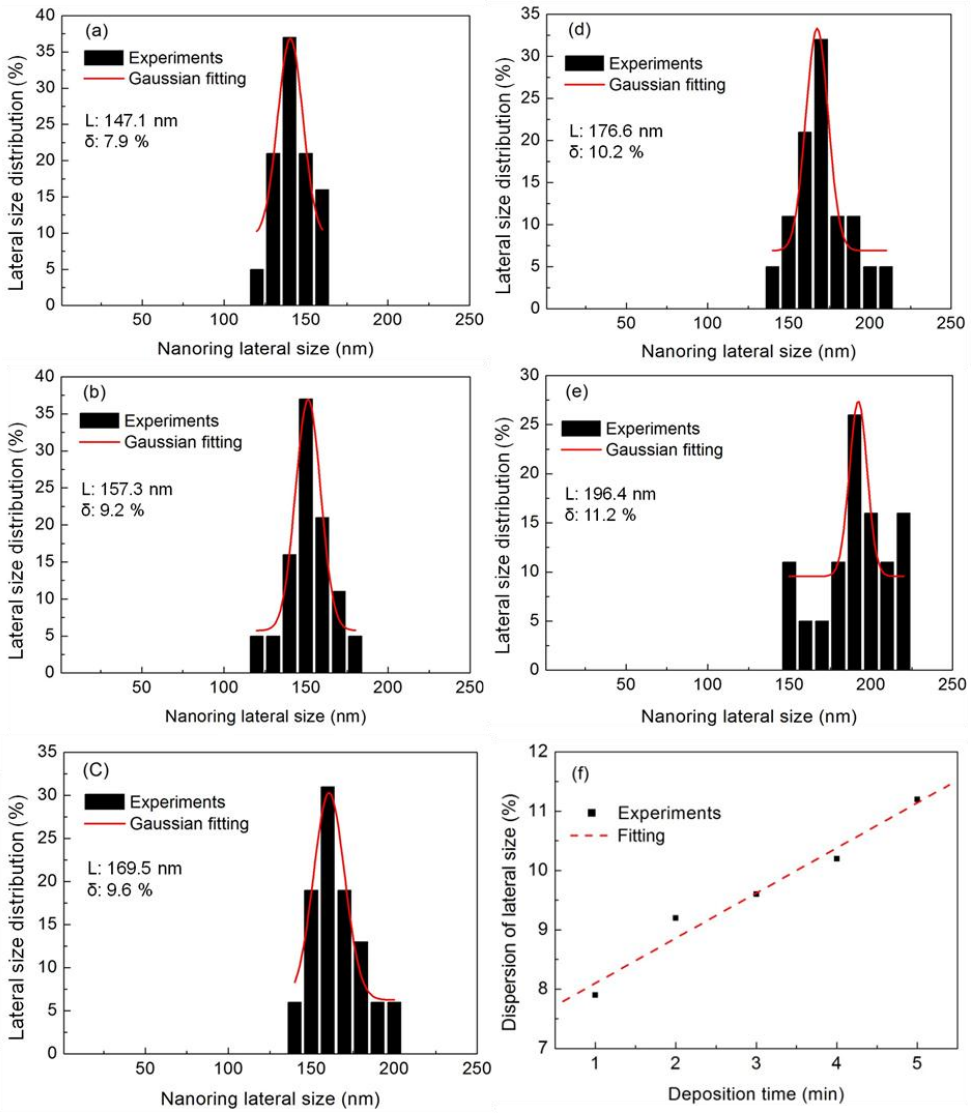

Fig. 5. The histograms show lateral size distribution of Cr nanoring with Cr thin film deposition time for (a) 1min, (b) 2 min, (c) 3 min, (d) 4 min, and (e) 5 min, respectively. (f) Relationship between dispersion of lateral size and Cr deposition time.

Fig. 6 shows that the lateral size and height of Cr nanorings increased proportionally with the deposition time. The measured growth rate of the Cr nanorings (or deposition rate of Cr film) is around 0.13 nm/sec. It is expected the lateral size and height of the Cr nanorings can be fine-tuned by the change of the deposition time.

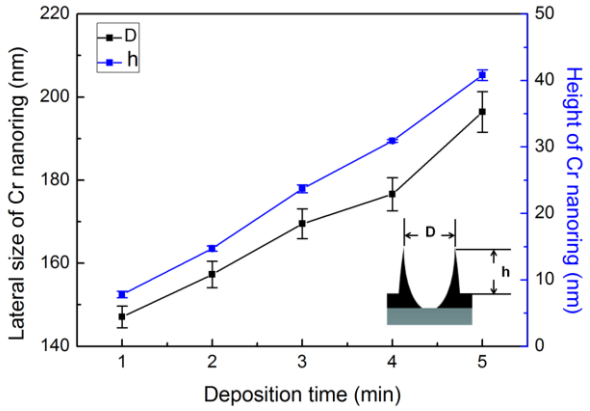

Fig. 6. Effect of deposition time on the lateral size and height of Cr nanorings.

The photoluminescence spectra of 100 nm Alq3 layer evaporated on the flat substrate and patterned substrate were shown in Fig. 7. Due to periodic structure of nanorings array, the extraction efficiency was enhanced 32.6% at a wavelength 525 nm compared to that of the flat substrate. And the full width half maximum (FWHM) was reduced from 116 nm to 81 nm, which the narrow emission wavelength favors improving the color purity. It is believed that the blue shift and improved light extraction behavior are related to the nano-structure induced quantum confinement effect [27-29]. It is expected that nanorings array based techniques can be applied for improving light extraction in display and lighting application.

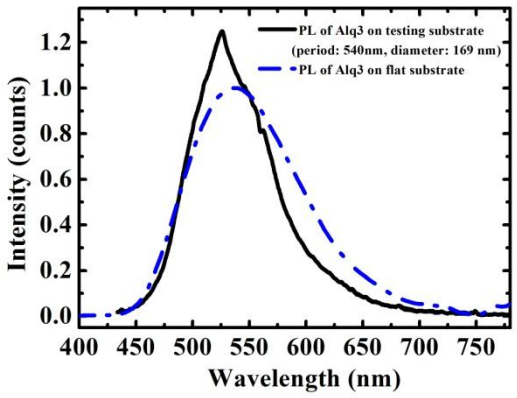

Fig. 7. Photoluminescence of Alq3 layer deposited on the testing substrate.

4. Conclusion

A lower cost and higher throughput fabrication process for obtaining the Cr nanoring arrays in long-ranged hexagonal order with controllable period by using nanosphere lithography (NSL) was investigated. The size of Cr nanorings can be easily controlled by RIE etching and Cr coating processes. The 32.6% luminous enhancement at a special wavelength of 525 nm and better color purity were observed in Cr nanorings structure.

Acknowledgement

This work was supported by the Institute of Materials Engineering, Ningbo University of Technology

References

[1] K. H. Li, Z. Ma, H. W. Choi, Appl. Phys. Lett. **98,** 071106 (2011).
[2] T. Yang, M. Hara, A. Hirohata, Appl. Phys. Lett. **90**, 022504 (2007).
[3] E. M. Larsson, J. Alegret, M. Kall, D. S. Sutherland, Nano Lett. **7**, 1256 (2007).
[4] M. E. Stewart, C. R. Anderton, L. B. Thompson, J. Maria, S. K. Gray, J. A. Rogers, R. G. Nuzzo, Chem. Rev. **108**, 494 (2008).
[5] C. Liu, V. Kamaev, Z. V. Vardeny, Appl. Phys. Lett. **86**, 143501 (2005).
[6] Y. H. Ho, K. Y. Chen, S. W. Liu, Y. T. Chang, D. W. Huang, P. K. Wei, Organic Electronics **12**, 961 (2011).
[7] J. G. Zhu, Y. Zheng, G. A. Prinz, J. Appl. Phys. **87**, 6668 (2000).
[8] X. Y. Ma, Nanotechnology **19**, 275706 (2008).
[9] J. Ye, M. Shioi, K. Lodewijks, L. Lagae, T. Kawamura, P. V. Dorpe1, Appl. Phys. Lett. **97**, 163106 (2010).
[10] T. Thio, H. F. Ghaemi, H. J. Lezec, P. A. Wolff, T. W. Ebbesen, J. Opt. Soc. Am. B, **16**, 1743 (1999).
[11] T. W. Ebbesen, H. J. Lezec, H. F. Ghaemi, Nature **391**, 667 (1998).
[12] H. F. Ghaemi, Tineke Thio, D. E. Grupp, T. W. Ebbesen, H. J. Lezec, Phys. Rev. B **58**, 6779 (1998).
[13] M. Faustini, M. Vayer, B. Marmiroli, M. Hillmyer, H. Amenitsch, C. Sinturel, D. Grosso, Chem. Mater. **22**, 5687 (2010).
[14] R. Marty, A. Arbouet, C. Girard, A. Mlayah, V. Paillard, V. K. Lin, S. L. Teo, S. Tripathy, Nano Lett. **11**, 3301 (2011).
[15] M. Kim, K. Kim, N. Y. Lee, K. Shin, Y. S. Kim, Chem. Commun. 2237 (2007).
[16] F. Yan, W. A. Goedel, Nano Lett. **4**, 1193 (2004).
[17] K. L. Hobbs, P. R. Larson, G. D. Lian, J. C. Keay, M. B. Johnson, Nano Lett. **4**, 167 (2004).
[18] H. W. Deckman, J. H. Dunsmuir, Appl. Phys. Lett. **41**, 377 (1982).
[19] N. D. Denkov, O. D. Velev, P. A. Kralchevsky, I. B. Ivanov, H. Yoshimura, K. Nagayama, Langmuir **8**, 3183 (1992).
[20] Y. H. Ye, F. LeBlanc, A. Hache, V. V. Truong, Appl. Phys. Lett. **78**, 52 (2001).
[21] L. Meng, H. Wei, A. Nagel, B. J. Wiley, L. E. Scriven, D. J. Norris, Nano Lett. **6**, 2249 (2006).

[22] X. Zu, X. Hu, L. A. Lyonc, Y. Deng, Chem. Commun. **46**, 7927 (2010).
[23] Y. K. Hong, H. Kim, G. Lee, W. Kim, J. I. Park, J. Cheon, J. Y. Koo, Appl. Phys. Lett. **80**, 844 (2002).
[24] E. M. Hicks, O. Lyandres, W. P. Hall, S. Zou, M. R. Glucksberg, R. P. Van Duyne, J. Phys. Chem. C, **111**, 4116 (2007).
[25] V. Zaporojtchenko, J. Zekonyte, S. Wille, U. Schuermann, F. Faupel, Nucl. Instr. and Meth. B **236**, 95 (2005).
[26] Y. J. Zhang, W. Li, K. J. Chen, J. Alloys Compd. **450**, 512 (2008).
[27] S. V. Gaponenko, Camebridge University Press. (1998).
[28] C. Delerue, G. Allan, M. Lannoo, J. Luminescence, **80**, 65 (1998).
[29] A. P. Alivisatos, Science **271**, 933 (1996).

*Corresponding author: hhchien@chu.edu.tw